Chapter V

Relation between
Surface Properties and Photoluminescence
Efficiency in CdSe Nanocrystals

Overview of the chapter:

The surface characteristics of colloidally synthesized CdSe nanocrystals with OPA and and those with OA have been explored with photoemission spectroscopy. We find that the amount of the unpassivated surface Se atoms of nanocrystals is related to the growth rates. Photoluminescence efficiency, furthermore, exhibits a strong dependence on the surface Se atoms with dangling bonds, suggesting that the lone-pair obitals at the nanocrystal surface play important roles in excitonic traps.

5.1 Introduction

Various organic ligands (e.g. TOPO and thiol) or semiconductor materials (e.g. CdS, ZnS and ZnSe) are used to provide the surface passivation of NCs. An effective surface passivation is known to prevent the fine particles from

oxidization and congregation and, more importantly, to improve the PL efficiency. Nanocrystallite materials such as $(ClO_4)\times 6H_2O$ capped CdSe NCs [1], thiols capped CdS NCs [2], and thiols capped CdTe NCs [3] have been studied on their structural properties. Detailed information about the surface/interface characteristics of these core/shell systems was very helpful in elucidating the optical behaviors. The properties of the fine materials are highly sensitive to the synthesis conditions: The size fractions corresponding to very low net growth rates (i.e., when growth and dissolution are almost in equilibrium) possess the highest PL quantum efficiencies and the best photostability. In contrast, the NCs grown under conditions far away from the equilibrium of growth have various defects giving rise to nonradiative recombination pathways [4,5]. It has been suggested that the former has a highly ordered surface thus less surface trapping states and the latter possess a rough surface.

Until now, however, the exact nature of the surface states providing nonradiative recombination pathways has not been fully clarified. Understanding of the surface states is therefore quite important for nanocrystals. Our motivation in this study is to comprehend how the surface properties of nanocrystals influence PL efficiency and the relationship between them.

5.2 Growth rate

The growth rates (The size evolution of growth time) of NCs prepared using OPA and those using OA are shown in Fig. 5.1, the vertical error bars represents the size distribution of NCs determined by TEM. Overall, we found that after the rapid initial growth of the nucleation stage to about 30 Å the growth of OA

prepared NCs slowed down substantially till 40 Å. In contrast, the NCs prepared using OPA had a relatively slower initial growth, while their subsequent growth was relatively faster compared to the OA-prepared NCs.
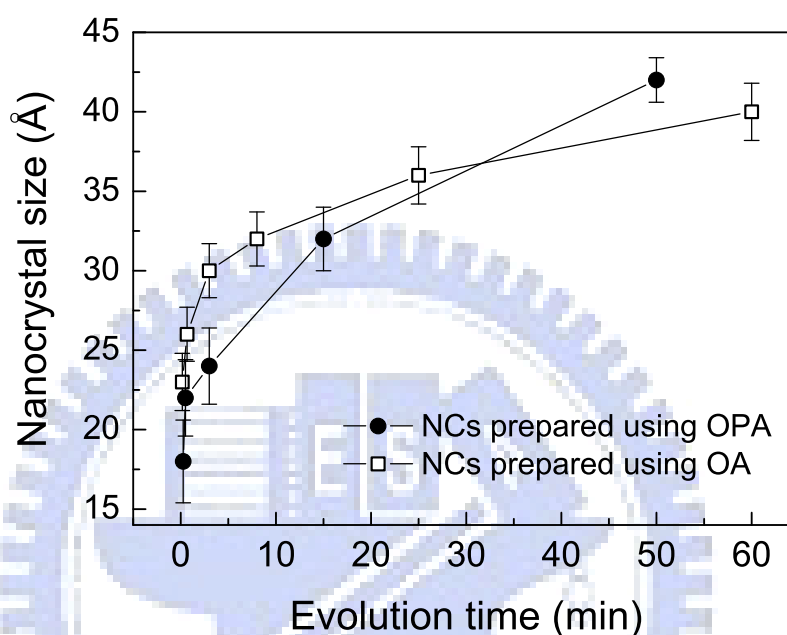

FIG. 5.1: The NC size as a function of evolution time during growth for NCs prepared using OPA and using OA.

5.3 Absorption and photoluminescence measurements

Figure 5.2 represents the evolution of the UV-absorption and PL spectra for CdSe NCs prepared by OA with a series of mean diameters D_m in the range from 23 to 40 Å. All of UV-absorption spectra possess up to five resolved exciton transitions and a sharp lowest energy peak (width of ~0.1 eV), reflecting narrow size distribution of CdSe NCs. Both the absorption and the PL spectra shift towards higher energy as the particle size decreases, which is contributed

from the effect of three-dimentional quantum confinement of the electrons within the NC.
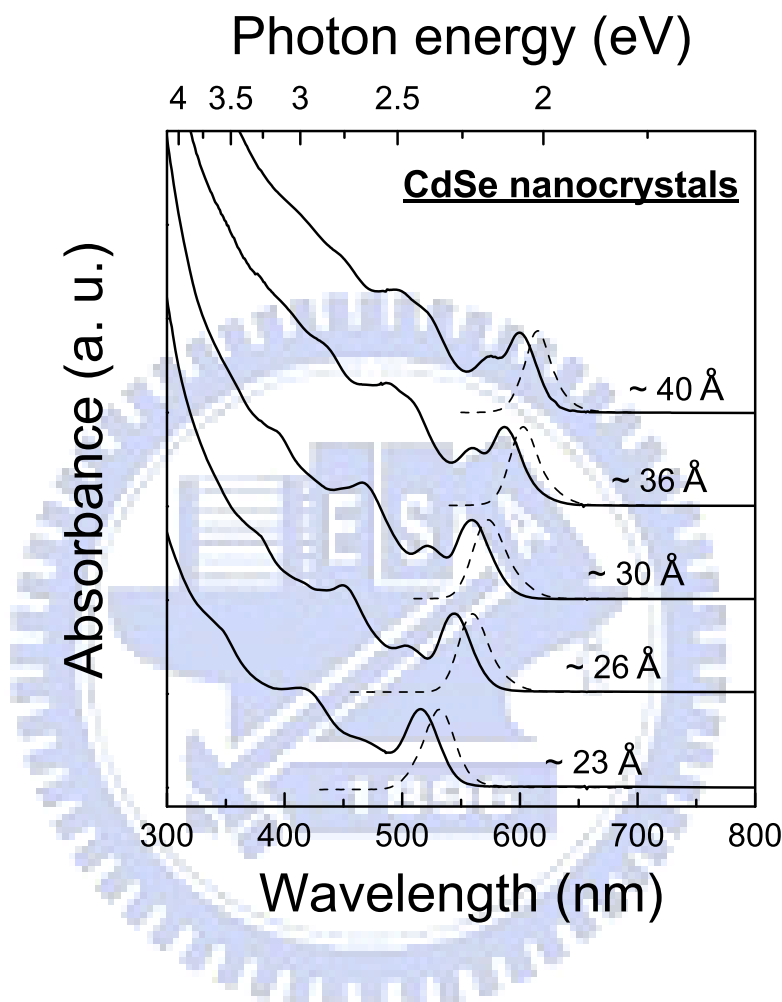
FIG. 5.2: Room temperature optical absorption and PL spectra of OA-prepared CdSe NCs dispersed in toluene.

Figure 5.3 shows the size dependence of the integrated PL intensity, normalized by absorbance at the excitation energy of the highest emission intensity, which approximately corresponds to the third absorption feature (for example, 420 nm for 23-Å NCs shown in Fig. 5.2), for OPA- and OA-prepared CdSe NCs. At higher excitation energies the absorbance contributed from the organic ligands increased steadily thus is not appropriate for normalization. The

NCs prepared using OPA exhibit a decreasing PL intensity with increasing size, the tendency is the same as described in the literature [6]; while OA prepared NCs have an increasing behavior similar to the result reported by Zhang *et al.* [7] The inset represents the absorption spectra of NCs, prepared by OPA and by OA, with the same size of 32 Å. The difference in the width of fine feature is possibly due to slightly larger size distribution of OPA-prepared NCs, compared to that of OA-prepared NCs, and/or their distinct surface structure.
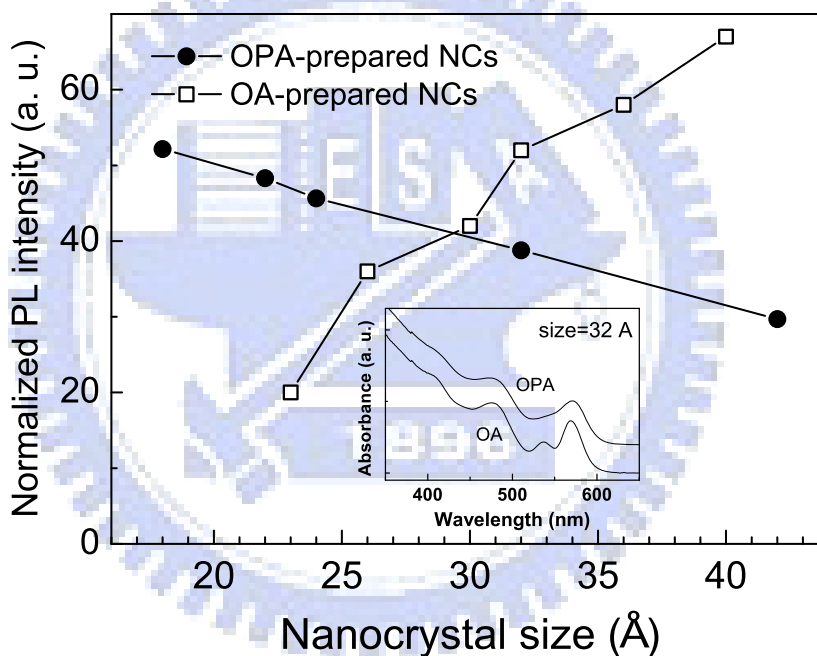

FIG. 5.3: The normalized PL intensity as a function of NC diameter for OPA- and OA-prepared NCs. Inset: The absorption spectra of OPA- and OA-prepared NCs with the sizes of 32 Å.

5.4 Photoemission studies

All core level spectra were recorded from a film of NCs and then fitted to the

minimum number of Voigt functions after the background removal adopting the polynomial function. The Fermi edge of gold was used to calibrate the energy scale of measured photoemission spectra.

5.4.1 Cd $3d_{5/2}$ level spectra
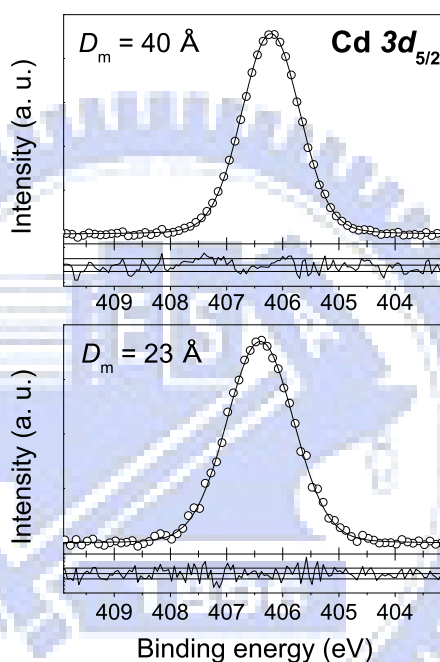
FIG. 5.4: Fits to the Cd $3d_{5/2}$ core-level photoemission spectra of OA prepared CdSe nanocrystals, with diameters of 40 and 23 Å, recorded at a surface sensitive energy of 480 eV.

The Cd $3d_{5/2}$ level photoemission spectra of OA-prepared CdSe NCs with diameters of 40 and 23 Å, recorded at an excitation energy of 480 eV, are shown in Fig. 5.4. The spectrum of 40 Å NCs can be well fitted with a single Voigt function, which has the binding energy of about 406.2 eV. The Gaussian width, which is related to the resolution of the experimental set-up, thermal broadening effect, as well as inhomogeneous broadening effects resulting from sample properties, is found to be 0.49 eV. The Lorentzian width, which is influenced by

lifetime effects, is turned out to be 0.064 eV. All fitting parameters are good accordance with the literature values [8].

For NC size of 23 Å the Cd $3d_{5/2}$ spectrum can also be well described by a fit with a single Voigt function, but exhibits a peak shift toward higher binding energy and a slight broadening (Gaussian width of ~0.57 eV) with respect to the 40 Å NCs. This energy shift was demonstrated as the increased ionization potential of small particles due to the final-state effect (see Chapter IV and Ref. 9), and the broader width of the photoemission peak for the smaller NCs can be related to a large variation of the bond angle within NCs observed from our EXAFS study discussed in Chapter III.

In addition, a single component observed in the $Cd_{5/2}$ level photoemission spectra, even for 23 Å NCs, indicates that the energy deviation between Cd−O/N and Cd−Se components is rather small and the experimental resolution is not sufficient to resolve this small core-level shift. It cannot be excluded that the unresolved surface component may be associated with different types of organic ligands bonding to different NC facets, which lead to an extreme broadening of the surface component (This lack of resolving surface components is consistent with reported binding energies of CdSe, CdS, CdO, and other compounds with a formal charge of 2+, Ref. 10).

Photoemission spectra of the Cd $3d_{5/2}$ core level for OPA-prepared CdSe NCs are shown in Fig. 4.1. All spectra can also be fit well by only one peak of Voigt function, which is the same as that observed for OA-prepared NCs; this can be expected since the identical surfactants were used in both preparation methods.

5.4.2 *Se 3d level spectra*
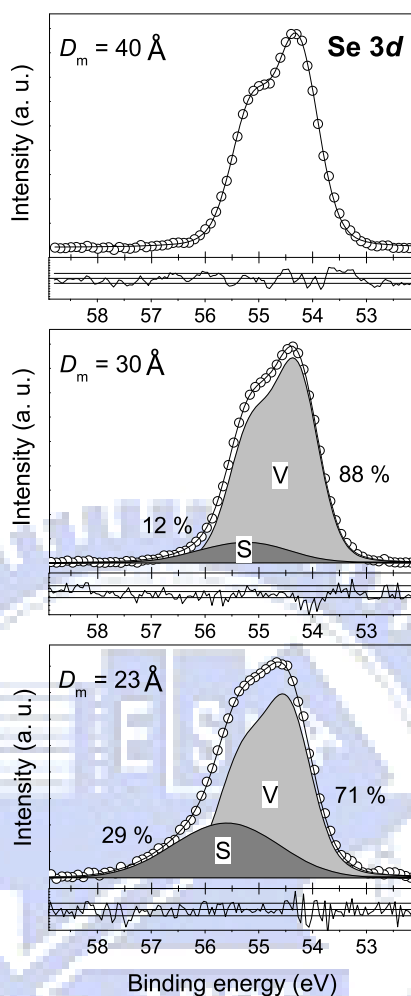
FIG. 5.5: Fits to the Se 3d core-level photoemission spectra of OA-prepared CdSe nanocrystals, with mean diameters of 40, 30, and 23 Å, recorded at a surface sensitive energy of 130 eV.

Figure 5.5 reveals the high-resolution Se 3d level photoemission spectra recorded at a surface sensitive energy of 130 eV and the corresponding fits; the excitation energy is chosen to keep the same probing depth for comparison with the Cd $3d_{5/2}$ level spectra above. Two spin-orbit split doublets of Voigt functions are required to obtain reliable fits to the Se 3d level spectra of CdSe NCs. As the NCs become smaller the intensity of the component (labeled "S") at higher binding energy is relatively enhanced with respect to that of another component

(labeled "V") at lower binding energy. For a given size, furthermore, the intensity of the "S" component became decreased relative to that of the "V" component using more bulk sensitive excitation energies [8]. It can therefore be assigned the component "S" to the contribution from the surface Se atoms, due to an increase of the S/V atoms ratio with decreasing size. The spin-orbit splitting is turned out to be 0.86±0.01 eV, which is consistent with the values reported in the literature.[8] The Lorentzian width is set to be identical for both components.

For 40-Å NCs a fit of good quality can be achieved with a single spin-orbit split doublet of Voigt functions. The Se $3d_{5/2}$ sublevel peak has a binding energy of 54.6 eV, in agreement with the previously reported value [8]. When the NC size is reduced, two components "S" and "V" are necessary to be included in the fits. The Se $3d_{5/2}$ sublevel of the component "V" for 30 Å CdSe NCs has a slight shift towards higher binding energy, as observed in our previous study on OPA-prepared CdSe NCs [9]. The Gaussian width is found to be 0.38 eV for component "V", while the value is 0.58 eV for component "S". This surface component has a shift of 0.67±0.06 eV toward higher binding energy compared to the volume component.

Our Se K-edge EXAFS studies, discussed in Chap. III, turned out that Cd atoms are the only first-nearest neighbors of Se atom, that is, the surface Se atoms are not bound to the capping organic ligands. In consequence, we associate the surface components observed in the Se $3d$ photoemission spectra with the unpassivated Se atoms at the NC surface. A rather broad surface component identified with the unpassivated surface Te atoms has been observed by Borchert *et al.* in a photoemission study of thioglycolic acid capped CdTe NCs [5]. The additional broadening of the surface component with respect to the

interior component was attributed to a rougher surface and various surface sites. In addition, we deem that the unpassivated surface Se atoms with dangling orbitals possess larger thermal fluctuations compared to the internal Se atoms, and it can likewise lead to an additional broadening of the surface component with respect to the volume component.

A fit of a reliable quality for the Se $3d$ spectrum of 23-Å CdSe NCs shows that the Gaussian widths of the component "V" and "S" have the magnitudes of 0.39 and 0.86 eV, respectively. Both of these components are broader than the corresponding components of 30 Å NCs. This indicates that the smaller dots have a more disordered structure of NCs with respect to larger dots, even in the interior of NC. Internal strain and disorder caused by competing relaxations from an irregular surface, even with strong chemical passivation, have been demonstrated using a PDF-based method [11]. Structural variations can modify electronic properties and should be the general feature of nano-scaled particle. Here we observe this structural modification in the interior of NCs with size on a study of high-resolution PS. Moreover, it is found that the broadening of the component "S" significantly increases as the decrease of NC size. This observation should be an indication of a highly disordered surface structure for small NCs, which is also an indication of surface reconstruction that have been discussed for InAs NCs [12]. In contrast, the variation in peak width of "V" component is less noticeable compared to that of "S" component with changing the NC size, indicating that the structural disorder observed in EXAFS study is primarily from the surface layer of NCs. It should be noted that not only the surface component is broader but also an observed surface component shift of 0.83±0.1 eV for 23-Å NCs is larger than those of 30-Å NCs. This increasing surface component shift is probably due to the changes in structural formation of

surface atoms such as a coordination number and distortion with NC size.

The Se 3*d* level photoemission spectra of OPA-prepared CdSe NCs are shown in Fig. 4.1. We should use two spin-orbit split doublets of Voigt functions to obtain satisfactory fits for all NC spectra. The observed surface component shift of OPA-prepared NCs almost corresponds to that of OA-prepared NCs, the component at higher bind energy would thus be assigned to the surface atoms of NCs with dangling bonds.

5.5 Discussion
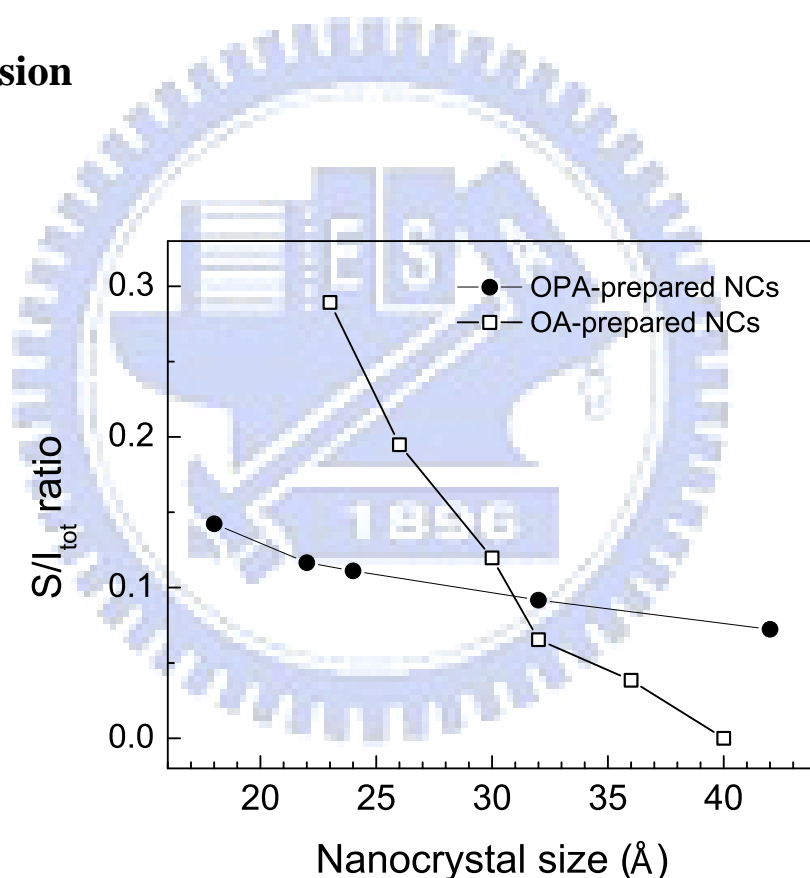
FIG. 5.6: The ratio of the surface component to total intensity determined from the Se 3*d* photoemission spectra of CdSe NCs prepared using OPA and OA as a function of size.

Figure 5.6 shows the surface component to total intensity (S/I_{tot}) ratio of the Se 3*d* photoemission spectra with respect to the NC size. Both ratios of NCs

prepared using OPA and OA exhibit an increasing behavior with the reduction in particle size. However, they have the quite different slopes of the size-dependent tendency. The NCs prepared with OA have a larger S/I_{tot} ratio and a broader width of the surface component "S" compared to OPA-prepared NCs below the size of ~30 Å, while the S/I_{tot} ratio becomes smaller when the size is larger than ~30 Å. This observation can be correlated with the growth rates of these two series of NCs (see in Fig. 5.1): a high growth rate can lead to a large amount of the unpassivated surface atoms with lone-pair orbitals and a rough surface; a low growth rate, in contrast, could give rise to an effective surface passivation and a highly ordered structure of NCs [5].
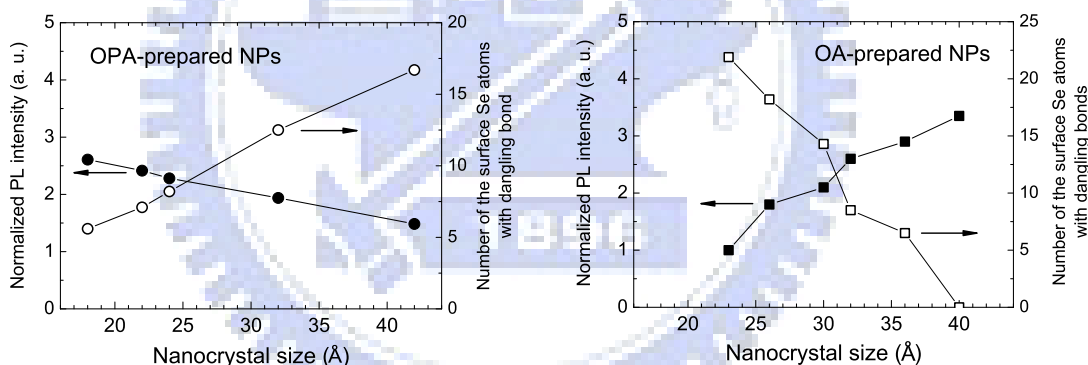
FIG. 5.7: The normalized PL intensity and number of the unpassivated surface Se atoms as a function of mean diameter for OPA- and OA-prepared NPs.

According to the S/I_{tot} ratio of the Se $3d$ photoemission spectra, we can determine the effective surface thickness considering the IMFP, which is related to the kinetic energy of the photoelectron, and further estimate the number of the unpassivated Se atoms. The size dependence of the surface Se atoms with dangling bonds is plotted in Fig. 5.7, for OPA- and OA-prepared CdSe NPs, together with that of the normalized PL intensity. Despite the normalized

intensities of these two samples have opposite size dependence of normalized PL intensity, it is obviously to see that, for both cases, the PL efficiency decreases as the number of the unpassivated surface Se atoms increases. This indicates that the PL efficiency has strong dependence on the unpassivated surface atoms of NPs.
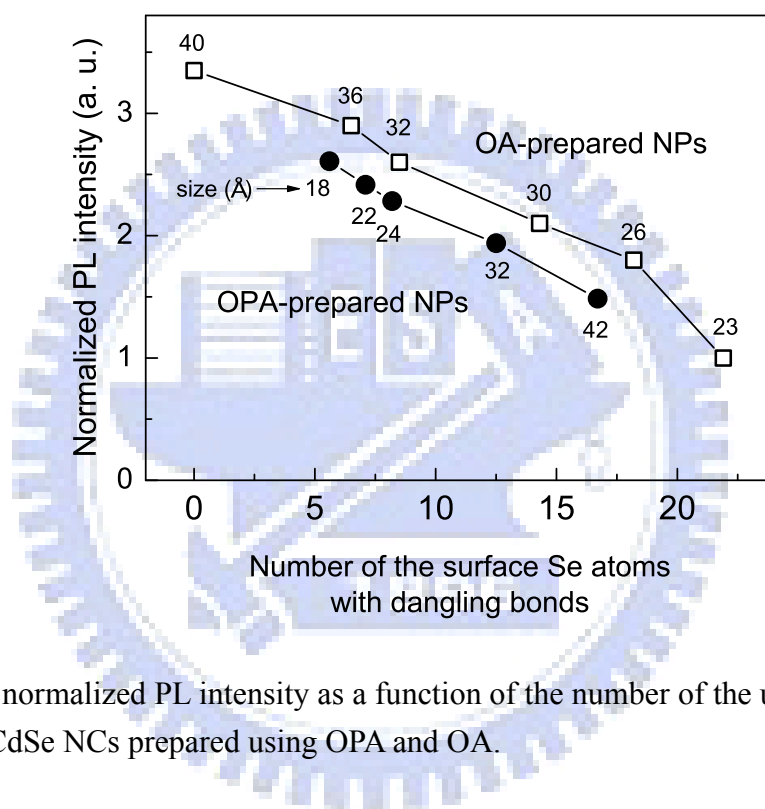
FIG. 5.8: The normalized PL intensity as a function of the number of the unpassivated surface Se atoms for CdSe NCs prepared using OPA and OA.

Figure 5.8 reveals the normalized PL intensity as a function of the number of the surface Se atoms with dangling bonds for OPA- and OA-prepared NPs. Surprisingly, they exhibit a quite similar behavior independent of the NP size. It has been shown in a theoretical calculation has shown that the unpassivated surface anions with dangling bond states play a critical role in trapping photoexcited hole [13]; this may lead to the behavior we observed in Fig. 5.8. However, the smaller particles possess the stronger quantum confinement and,

thus, have a higher luminescent quantum yield [14]. When the particle size becomes smaller, furthermore, the probability of the coupling between the wave function of the photoexcited hole and the lone-pair orbitals at the NP surface would increase. As a result, a puzzled problem about the size-independent behaviors shown in Fig. 5.8 remains to be resolved.

5.5 Summary

High-resolution photoemission studies combined with EXAFS results for colloidally prepared CdSe NCs provide the information of the surface properties, in which the Cd atoms at the NC surface are bonded to the terminated atoms of organic ligands, while most of the surface Se atoms remain unpassivated. That the dangling bonds and structural disorder at the NC surface might lead to nonradiative recombination pathways could be used to elucidate the observed PL efficiency. However, we found that PL efficiency is solely related to the surface atoms with dangling bonds but independent on the particle size, which remains a puzzled result to be resolved.

5.6 References

[1] A. C. Carter, C. E. Bouldin, K. M. Kemmer, M. I. Bell, J. C. Woicik, and S. A. Majetich, Phys. Rev. B **55**, 13822 (1997).

[2] J. Rockenberger, L. Troger, A. Kornowski, T. Vossmeyer, A. Eychmuller, J. Feldhaus, and H. Weller, J. Phys. Chem. B **101**, 2691 (1997).

[3] J. Rockenberger, L. Troger, A. L. Rogach, M. Tischer, M. Grundmann, A.

Eychmuller, and H. Weller, J. Chem. Phys. **108**, 7807 (1998).

[4] D. V. Talapin, A. L. Rogach, E. V. Shevchenko, A. Kornowski, M. Haase, H. Weller, J. Am. Chem. Soc. **124**, 5782 (2002).

[5] H. Borchert, D. B. Talapin, N. Gaponik, C. McGinley, S. Adam, A. Lobo, T. Möller, and H. Weller, J. Phys. Chem. B **107**, 9662 (2003).

[6] P. Reiss, J. Bleuse, and A. Pron, Nano Lett. **2**, 781 (2002).

[7] J. Y. Zhang, X. Y. Wang, M. Xiao, L. Qu, and X. Peng, Appl. Phys. Lett. **81**, 2076 (2002).

[8] H. Borchert, D. V. Talapin, C. McGinley, S. Adam, A. Lobo, A. R. B. de Castro, T. Möller, and H. Weller, J. Chem. Phys. **119**, 1800 (2003).

[9] P. J. Wu, K. D. Tsuei, K. H. Wei, and K. S. Liang, Solid State Commun. **141**, 6 (2007).

[10] J. F. Moulder, W. F. Stickle, P. E. Sobol, and K. D. Bomben, *Handbook of X-ray Photoelectron Spectroscopy* (Perkin-Elmer, Eden Prairie, Minnesota, 1992).

[11] B. Gilbert, F. Huang, H. Zhang, G. A. Waychunas, and J. F. Banfield, Science **305**, 651 (2004).

[12] C. McGinley, M. Riedler, and T. Möller, Phys. Rev. B **65**, 245308 (2002).

[13] H. Fu and A. Zunger, Phys. Rev. B **56**, 1496 (1997).

[14] N. Pauc, V. Calvo, J. Eymery, F. Fournel, and N. Magnea, Phys. Rev. B **72**, 205325 (2005).